ISBN: 978-3-95450-248-6 ISSN: 2673-5490 doi: 10.18429/JACoW-IPAC2025-TUPM015

DESIGN STUDY FOR A TRANSVERSE DEFLECTING CAVITY BASED DE-CHIRPER

A. DeSimone*, G.Ha, Northern Illinois University, DeKalb, USA
S. Doran, W. Liu, J. Power, E. Wisniewski[1], Argonne National Laboratory, Lemont, USA
Q. Marksteiner, H. Xu, N. Yampolsky, Los Alamos National Laboratory, Los Alamos, USA
[1]also at Illinois Institute of Technology, Chicago, USA

Abstract

This study proposes a method of particle beam longitudinal chirp control by using transverse deflecting cavities and negative identity drift sections. Using the same beamline design as a cavity-based chirper, it has been shown that a de-chirper can be made by altering the drift sections between deflecting cavities to form negative drift sections. Two methods of producing these negative drift sections used three and five quadrupoles. The three-quadrupole approach does not work, as it results in large beam sizes and emittance in one of the transverse planes; five quadrupoles is also not feasible due to experimental resource constraints and spatial limitations. A new proposed de-chirping method is to use three quadrupoles to make a negative identity drift section instead of a negative drift section between the cavities. Simulations have been performed to verify the de-chirping ability of this negative identity drift design for a deflecting cavity-based de-chirper.

INTRODUCTION

Longitudinal chirp is often controlled by operating the main linac at off-crest phases. Although this linac phase control effectively adjusts the longitudinal chirp, it introduces significant loss of beam energy compared to the on-crest operation. This could also result in more expansive building and operation costs. Currently, a collaboration is underway to address this issue and imposing a large chirp without linac phase control.

The key idea utilizing a transverse deflecting cavity (TDC) was proposed by Ref. [1]. Three TDCs arranged in series with appropriate spacing and strengths can impose a negative chirp to the beam. However, this design does not allow for a positive chirp to be imparted. A modification is required to make the chirper beamline also working as a de-chirper. In this paper, we discuss a design for a TDC-based de-chirper that shares the same TDC configuration as a chirper, with modified drift sections.

LONGITUDINAL CHIRP CONTROL VIA TDC-BASED BEAMLINE

In this section, we start with a brief review of the TDC-based chirping. Then, the dechirping will be discussed.

Imposing Negative Longitudinal Chirp

Three TDCs configured as Fig. 1 can adjust the longitudinal chirp to be more negative than the initial condition. The change of the chirp Δh corresponds to the R_{65} of the transfer matrix. In the case of the chirper, it is given by,

$$R_{65} = -\frac{2}{3}\kappa^2(3D + 2L_{\mathrm{TDC}}), \quad (1)$$

where κ is the deflecting cavity kick strength, D is the distance between two TDCs. This equation assumes equal spacing between the TDCs.

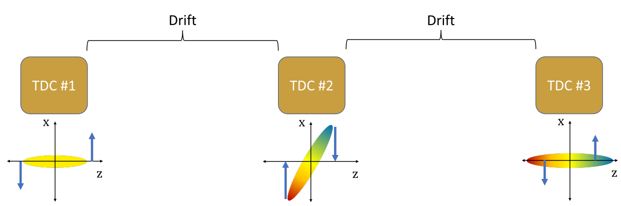

Figure 1: Schematic layout of the chirper beamline. The orange boxes are transverse deflecting cavities.

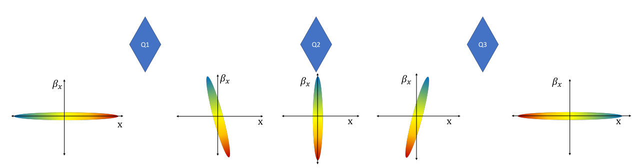

Figure 2: Negative identity drift configuration and corresponding beam evolution. The blue diamonds represent quadrupole magnets.

According to this matrix calculation, R_{65}, which corresponds to the change in the chirp, is proportional to κ^2. Thus, simply flipping the kicking direction of the TDC does not equate to changing the sign of the chirp. This result also shows a valid approach to make a positive chirp. When the drift length satisfies,

$$D < -\frac{2}{3}L_{\mathrm{TDC}}, \quad (2)$$

The chirp will be shifted to more positive value. Such negative drift length can be achieved by properly optimizing five quadrupole magnets. However, the implementation of five quadrupoles is costly, and the tuning procedure is not straightforward. While forming a negative drift with three quadrupoles has also been considered, it was shown to be impractical due to a significant increase in the beam size of the non-kicking plane.

* z2035090@students.niu.edu

ISBN: 978-3-95450-248-6 ISSN: 2673-5490 doi: 10.18429/JACoW-IPAC2025-TUPM015

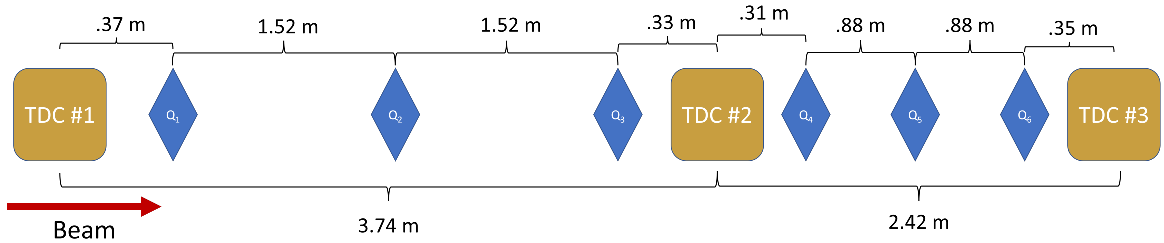

Figure 3: Layout of de-chirper beamline. The orange boxes are TDCs and the blue diamonds are quadrupoles.

Imposing Positive Longitudinal Chirp

Instead of using negative drift, we propose a different approach using negative identity transport that can be produced by three quadrupoles. The negative identity section's transverse matrix is given by,

$$R = \begin{pmatrix} -1 & D \\ 0 & -1 \end{pmatrix}. \tag{3}$$

Here, the first and the third quadrupole focus the beam to the interested plane and form the negative identity transport. The middle quadrupole focuses the other plane so that we can manage the entirety of the transverse optics. The transverse phase space will be flipped after this section as shown in Fig. 2.

When a negative identity section is placed after the first TDC, the transverse kick imparted by the first TDC will essentially be reversed—equivalent to changing the sign of the TDC strength. Then, the middle TDC, with large transverse beam size from coupling with z-coordinate, imparts the z-δ correlation. Here the orientation of the correlation will be opposite to the chirper. Then, the second negative identity drift flips the transverse phase space again, which compensates the impact of the first negative identity transport. Lastly, the third TDC removes remaining x-z coupling. The R_{65} of this beamline is,

$$R_{65} = \frac{\kappa^2}{2}(-L_{\mathrm{TDC}} + 4D). \tag{4}$$

A positive chirping will be provided as long as the condition $D > L_{\mathrm{TDC}}/4$ is met.

VERIFICATION OF DE-CHIRPING BY PARTICLE TRACKING SIMULATION

To verify the efficacy of the de-chirper design, the transport of an ideal 6D-Gaussian beam was simulated using GPT code [2]. The 6D Gaussian beam was generated with initial beam parameters given in Table 1. The beamline layout is provided in Fig. 3 The field map of deflecting cavity in Ref. [3] was implemented in the simulation. Quadrupole strengths to form negative identity transport were from transfer matrix-based optimization. The resulting longitudinal phase space before and after the de-chirper is shown in Fig. 4. A beam having initially zero chirp obtained a positive chirp at the end of the de-chirper.

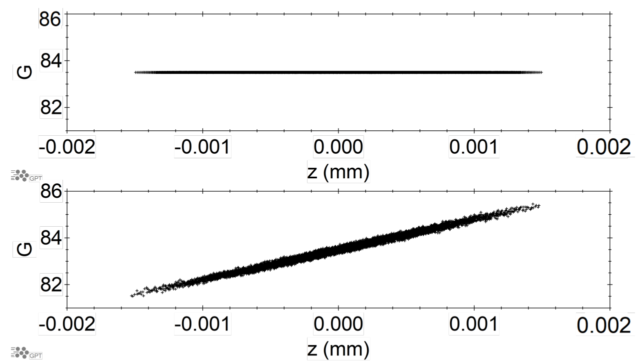

Figure 4: Simulated longitudinal phase space before and after a de-chirper.

It is worth nothing that we observed a significant increase in uncorrelated energy spread. This originates from the second order effects due to large energy spread rather than remaining transverse-longitudinal couplings.

Table 1: Nominal Initial Beam Conditions

Beam parameters	Values
$\epsilon_{n,x}$, $\epsilon_{n,y}$	1 um
σ_x, σ_y	1 mm
σ_z	0.5 mm
$\sigma_{x'}$, $\sigma_{y'}$	10 urad
σ_δ	10 urad
S_y,S_z	$0\,\mathrm{m}^{-1}$
S_x	$-0.3\,\mathrm{m}^{-1}$

INPUT BEAM PARAMETER SCAN TO ESTIMATE SECOND ORDER EFFECTS

We scanned initial slopes (S_x, S_y, S_z) to estimate the second order effects on the final normalized emittances. Nominal initial beam conditions and parameter scan ranges are listed in Table 1 and Table 2. Because numerical solvers were used to find the strengths of the quadrupoles and TDCs, there are multiple solutions producing the negative identity drift with different horizontal optics. Table 3 summarizes TDC and quadrupole strengths used in the simulations. Quadrupoles had hard edges and effective length of

ISBN: 978-3-95450-248-6 ISSN: 2673-5490 doi: 10.18429/JACoW-IPAC2025-TUPM015

Table 2: Parameter Scan Ranges

Beam parameters	Range
S_x, S_y	[-1, 1] m^{-1}
S_z	[-15, 15] m^{-1}

Table 3: Element Strengths

Beamline parameters	Values
Q_1, Q_3	-0.95 $T{\cdot}m^{-1}$
Q_2	0.97 $T{\cdot}m^{-1}$
Q_4, Q_6	-1.65 $T{\cdot}m^{-1}$
Q_5	1.51 $T{\cdot}m^{-1}$
TDC_1	1.13 m^{-1}
TDC_2	3.38 m^{-1}
TDC_3	2.14 m^{-1}

L_Q = 0.1 m. It is also worth noting that the maximum step size of 10 ps was used to ensure simulation convergence.

The result of slope-scan is shown in Fig. 5 through Fig. 7. Note that TDCs kick the beam in the y-direction. For each 2D contour plot, we selected the remaining slope to give minimum emittance. It is clear that there are strong slope dependencies, which most likely originate from the second order effects. While the horizontal slope has minimal impact on the emittance, the vertical slope is the most sensitive. In general, a non-optimal slope in the TDC kicking direction seems having the largest impact on the final emittances. Further analysis will be required, but properly matching the beam condition would minimize these emittance growths.

FUTURE WORK

The preliminary result offers insight into the behavior of the proposed de-chirper design—most notably, the strong second-order effects. Further analysis is necessary to confirm the severity of these effects and to investigate methods of suppressing them.

In addition, to assess the utility and capabilities of the de-chirper, a study on space charge effects must be conducted. There is a concern that strong focusing from the quadrupoles forming the negative identity introduces a locally high density, which may introduce space-charge induced aberrations.

Once the analysis on the second order effects and the space-charge effects are completed, start-to-end simulations will be performed to prepare the experimental demonstration of the de-chirper.

ACKNOWLEDGMENTS

This research is supported by the U.S. Department of Energy through the Laboratory Directed Research and Development program of the Los Alamos National Laboratory under project number 20240231ER and the Department of Energy, Office of High Energy Physics, under Contract No. DE-AC02-06CH11357.

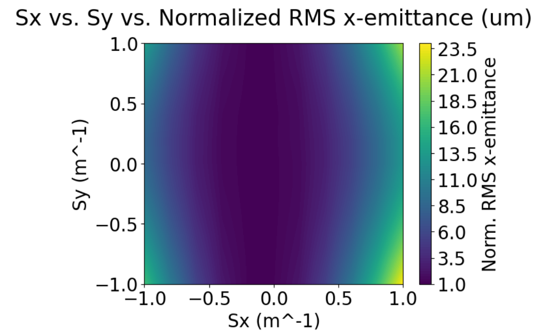

Figure 5: Final horizontal emittance vs. vertical slope vs. longitudinal slope.

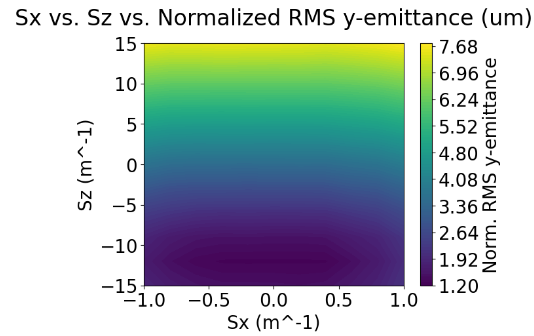

Figure 6: Final vertical emittance vs. horizontal slope vs. longitudinal slope.

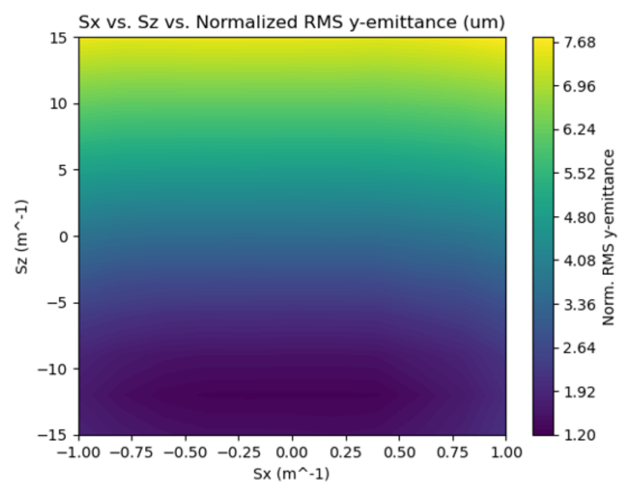

Figure 7: Final horizontal emittance vs. vertical slope vs. longitudinal slope.

REFERENCES

[1] N. Yampolsky, E. I. Simakov, and A. Malyzhenkov, "Imposing strong correlated energy spread on relativistic bunches with transverse deflecting cavities", *Phys. Rev. Accel. Beams*, vol. 23, no. 5, p. 054 403, 2020.

[2] S. B. van der Geer and M. J. de Loos, *Gpt user manual*. https://www.pulsar.nl/gpt/

[3] P. Piot *et al.*, "Commissioning of a 1.3-GHz Deflecting Cavity for Phase-Space Exchange at the Argonne Wakefield Accelerator", in *Proc. IPAC'12*, New Orleans, LA, USA, May 2012, pp. 3350–3352. https://jacow.org/IPAC2012/papers/THPPC031.pdf